Journal of Multidisciplinary Engineering Science and Technology (JMEST)
ISSN: 2458-9403
Vol. 8 Issue 5, May - 2021

Unsteady Newtonian fluid flow from an open rectangular reservoir with an orifice

Noarijaona RATOVONARIVO*
Laboratory of Mechanics Energy and Environment (LMEE)
University of Fianarantsoa
Madagascar
tovnarivo@yahoo.fr

Marcelin Hajamalala ANDRIANANTENAINA
Laboratory of Mechanics Energy and Environment (LMEE)
University of Fianarantsoa
Madagascar
hajamalalaa@yahoo.fr

Belkacem ZEGHMATI
Laboratory of Mathematics And Physics (LA.M.P.S),
University of Perpignan Via Domitia,
France

zeghmati@univ-perp.fr

***Abstract*— The aim of this work is to study the numerical two-dimensional unsteady Newtonian fluid flow an open rectangular reservoir with an orifice without heat, mass transfer and volume variation.The governing equations of fluid flow are based on the continuity equation and the Navier-Stokes equations. The numerical solution is obtained by discretizing the governing equations using the finite-volume technique.Thomas algorithm has been used to solve the algebraic equations system.The Semi Implicit Method for Pressure Linked Equations algorithm was introduced to couple the velocity-pressure. A numerical code was developed.A parametric study was carried out to determine the effects of several parameters on the velocity and pressure of the liquid during the flow in the reservoir. It is found that the velocities, the fluid pressure and the Reynolds number depend essentially on the size of the reservoir. An impact of time on the parameters has been investigated. To validate the model, comparison between the present work results with the analytical results of Poiseuillein the case where the width of the orifice and that of the reservoir are comparable. The results show good agreement with those of the literature.**

Keywords—modeling; navier stokes equations; Newtonian fluid; rectangular; reservoir

I. INTRODUCTION

The reservoir plays the role of storage. It is presented in different shape, particularly opened or closed cubic, parallelepiped and cylindrical. It usually has input and output which may or may not operate at the same time depending on its use. If the diameter of the reservoir is very large compared to its height, we have a horizontal reservoir called a shallow reservoir, but in the opposite case, it is the vertical reservoir or deep reservoir [1].This system can often be found in various industrial applications such as the food industry, the petroleum industry and especially the hydroelectric industry to store liquid. Because of its wide applications, many researchers direct their research work on the study of this system. There are two types of fluid draining such as single-layer draining which was developed numerically by Zhou and double-layer draining which was studied experimentally and analytically by Lubin&Springer and Forbes et al. [2].The lower, denser fluid flows at constant velocity through a finite-width drain hole in the bottom of the reservoir. The upper lighter fluid is recharged at the top of the reservoir, with a corresponding inlet volume flow and the outward flowthrough the drain. As a result, the interface between the two fluids moves evenly downward, and is eventually pulled out through the drain hole.The work of Fadhilah et al. [3] focused on the numerical simulation of the flow of a liquid in a cylindrical reservoir. They determine the fluid drain time in this reservoir using open FOAM which is an open source CFD package.

Matthieu et al. [4] has experimentally and numerically studied the flow and deposition of sediments in shallow rectangular basins, which consists upstream in a sudden widening and downstream in a sudden narrowing. His work aims to establish a classification of flows that can take place in basins and to determine the influence of the flow on the location of deposits and on the efficiency of settling. To model his system, he uses the two-dimensional Colebrook-type Saint Venant equation and the Wolf finite volume method.

Flow velocity and sedimentation patterns in shallow rectangular reservoirs with different asymmetric inlet and outlet channel locations have been investigated experimentally and numerically by Camnasio et al. [5]. Velocity fields were measured throughout the reservoir, both for water flow and for sediment. The experimental results were compared to numerical simulations performed with the Wolf 2D depth-averaged flow model, using a k-ε turbulence model. Kantoush et al. [6] also conducted suspended load experiments, which investigated reservoir geometries characterized by a symmetrical position of the inlet and outlet channels, but with varying reservoir length and width. The sediment deposition pattern was measured using an echo sounder and empirical relationships were established to predict the influence of reservoir geometry on trapping efficiency. He concludes that numerical simulations of flow in shallow rectangular reservoirs mainly focus on low and moderate Reynolds numbers, for which the

symmetry of the flow can be broken as the Reynolds number increases. The study by Taymazet al. [7], deals with the three-dimensional numerical modeling of the flow field in shallow reservoirs. It focuses on the numerical modeling of the velocity field in shallow reservoirs with flat and deformed beds. A fully 3D digital model using the finite volume method was used to determine the flow velocity field. Their results can be used to optimize the design of sand traps or water storage facilities, and also to optimize sediment management in reservoirs. Flow in a shallow reservoir with varying inlet and outlet positions was considered by Ferrara et al. [8]. Using numerical simulations, a systematic analysis was performed of the influence of the location of the inlet and outlet on the flow fields developing in shallow rectangular reservoirs of various sizes. Depending on the relative location of the inlet and outlet with respect to the axis of the reservoir, contrasting flow patterns are obtained. The results also reveal the appearance of bistable flow patterns. Daniel Augusto de Miranda et al. [9] made experimental and numerical studies of flow patterns in shallow rectangular reservoirs with symmetrically placed inlet and outlet channels. This work aims to analyze the flow models in a rectangular reservoir with upstream and downstream channels placed symmetrically, taking into account three different flows in constant flow regime. Experimental tests were carried out in a prototype laboratory, consisted of a reservoir 3.0 m long and 2.0 m wide, with a maximum depth of 0.30 m. In addition, it was applied the WOLF 2D software for numerical modeling.

The work of Peng et al. [10] focused on the modeling of free surface flow in a shallow rectangular basin using the Lattice Boltzmann method. Asymmetric flows occurring in basins with different length-to-width ratios are simulated. The effects of Froude number and bed friction on flow asymmetry and tie length are investigated. The results show that the flow becomes less asymmetrical and the re-coupling length increases with the increase in the Froude number or the friction of the bed.

All this shows that the work that is already done on the rectangular reservoir has been based either on its emptying, or on its study in the shallow case. For the present work, it focuses on the two-dimensional, laminar and unsteady flow of a Newtonian fluid in an open rectangular reservoir with an orifice placed asymmetrically on the bottom using the NavierStokes equation and the finite volume method in the case where the fluid mass flow rate is constant.

II. GOVERNING EQUATIONS

A. *Physical description*

The schematic of the rectangular reservoir filled with water, permanently supplied from the outside, of internal width L and height H that is emptied using an orifice of width l.The flows entering and leaving the reservoir are proportional so that the fluid level is constant Fig.1. Fluid flow in rectangular reservoir has been considered. The flows are two-dimensional and laminar. The flows are stationary and heat and mass transfers are negligible. The force exerted on this fluid is only the force due to the gravity field. The physical properties of water are assumed constant and the water level in the reservoir is almost constant. The flow of water leaving the reservoir is assumed constant.

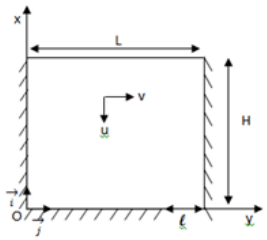

Figure 1. Schematic diagram of rectangular

B. *Equations*

Therefore, the steady state governing equations describing fluid flow in the reservoir in the cartesian coordinates are as follows:

Continuity equation:

$$\frac{\partial u}{\partial x}+\frac{\partial v}{\partial z}=0 \tag{1}$$

Navier Stokes equations :

$$\begin{cases}\dfrac{\partial u}{\partial t}+u\dfrac{\partial u}{\partial x}+v\dfrac{\partial u}{\partial y}=-\dfrac{1}{r}\dfrac{\partial P}{\partial x}+\dfrac{m}{r}\left(\dfrac{\partial^2 u}{\partial x^2}\right)+\dfrac{\partial^2 u}{\partial y^2}+g\\ \dfrac{\partial v}{\partial t}+u\dfrac{\partial v}{\partial x}+v\dfrac{\partial v}{\partial y}=-\dfrac{1}{r}\dfrac{\partial P}{\partial y}+\dfrac{m}{r}\left(\dfrac{\partial^2 v}{\partial x^2}\right)+\dfrac{\partial^2 v}{\partial y^2}\end{cases} \tag{2}$$

Where P represents the fluid total pressure, ρ being the fluid density, μ the dynamic viscosity of the fluid, g the gravity acceleration and t is the times.

C. *Boundary conditions:*

- At the reservoir outlet

$$\begin{cases}\text{For } x=0,\ 0\le y\le L-l \text{ and } 0\le t\le T\\ T=\dfrac{S}{s}\sqrt{\dfrac{2H}{g}};\ S=\dfrac{pD^2}{4} \text{ and } s=\dfrac{pd^2}{4}.\\ u(0,y,t)=0;\\ v(0,y,t)=0;\end{cases} \tag{3}$$

Where L denotes the reservoir width, l being the orifice width, S the reservoir section, s the orifice section and T is the emptying time.

$$\begin{cases}\text{For } x=0,\ L-l\le y\le L \text{ and } t=T\\ u(0,y,T)=-U_0 \text{ with } U_0=\sqrt{2gH}\\ v(0,y,T)=0;\\ P(0,y,T)=P_{atm};\end{cases} \tag{4}$$

Where U_0 gives the average fluid velocity at the outlet and P_{atm}being the atmospheric pressure.

- At the reservoir inlet :

$$\text{For } x = H,\ 0 \pounds y \pounds L \text{ and } t = 0 \quad \begin{cases} u(H, y, 0) = 0; \\ v(H, y, 0) = 0; \end{cases} \tag{5}$$

H is the reservoir height.

- On the walls:

Left wall:

$$\text{Pour } y = 0,\ 0 \text{p } x \text{p } H \text{ et } 0 \text{p } t \text{p } T \quad \begin{cases} u(x, 0, t) = 0; \\ v(x, 0, t) = 0; \end{cases} \tag{6}$$

Rightwall :

$$\text{Pour } y = L,\ 0 \text{p } x \text{p } H \text{et } 0 \text{p } t \text{p } T \quad \begin{cases} u(x, L, t) = 0; \\ v(x, L, t) = 0; \end{cases} \tag{7}$$

D. Numerical methodology

These eq. (1) and eq. (2), associated with boundary conditions (eq. (3) to eq.(7)) must make adimensional to show the Reynolds number and the Froude number that characterizes the flow regime. One adopt the following adimensionalization:

$$x^+ = \frac{x}{D_H};\ y^+ = \frac{y}{D_H};\ u^+ = \frac{u}{U_0};\quad v^+ = \frac{v}{U_0};\ P^+ = \frac{P - P_{atm}}{\rho U_0^2};\ t^+ = \frac{U_0 t}{D_H} \tag{8}$$

Where x^+ is the dimensionless abscissa, y^+being the dimensionless ordinate, u^+ the dimensionless velocity follow x^+, v^+ the dimensionless velocity follow y^+, P^+ the dimensionless pressure, t^+ the dimensionless time and D_H the hydraulic diameter.

$$D_H = \frac{4s}{p} \tag{9}$$

Wheres the orifice section and p perimeter of the orifice

Dimensionlesscontinuityequation:

$$\frac{\partial u^+}{\partial x^+} + \frac{\partial v^+}{\partial y^+} = 0 \tag{10}$$

Dimensionless Navier Stokes equation:

$$\begin{cases} \frac{\partial u^+}{\partial t^+} + u^+ \frac{\partial u^+}{\partial x^+} + v^+ \frac{\partial u^+}{\partial y^+} = -\frac{\partial P^+}{\partial x^+} + \\ \frac{1}{Re}\left[\frac{\partial^2 u^+}{\partial x^{+2}} + \frac{\partial^2 u^+}{\partial y^{+2}}\right] - \frac{1}{Fr^2} \\ \frac{\partial v^+}{\partial t^+} + u^+ \frac{\partial v^+}{\partial x^+} + v^+ \frac{\partial v^+}{\partial y^+} = -\frac{\partial P^+}{\partial y^+} + \\ \frac{1}{Re}\left[\frac{\partial^2 v^+}{\partial x^{+2}} + \frac{\partial^2 v^+}{\partial y^{+2}}\right] \end{cases} \tag{11}$$

$$Re = \frac{\rho U_0 D_H}{\mu} \tag{12}$$

$$\nu = \frac{\mu}{\rho} \tag{13}$$

Where Re is the Reynolds number, Fr being the Froude number and υ the fluid kinematic viscosity.

These Eq. (10) and Eq. (11) are discretized using the finite volume method and the Pantakar technique [11, 12]. The general form is written as follow:

$$A_{i,j} F_{i,j-1} + B_{i,j} F_{i,j} + C_{i,j} F_{i,j+1} = D_j \tag{14}$$

Φmay be the dimensionless velocities u^+, or the speed v^+, or the dimensionless pressure P^+. The adequacy between the velocity and pressure fields is ensured by the SIMPLE algorithm.

The systems of algebraic equations thus obtained are solved using the algorithm of Thomas and Gauss.

- Shear stress

The shear stress is defined by:

$$t(x, y) = m \frac{\partial u(x, y)}{\partial y} \tag{15}$$

τ represents the shear stress in Pascal (Pa)

Where : with $t = t^+ m \frac{U_0}{D_H}$ t^+ is the dimensionless shear stress

$$t^+(x^+, y^+) = \frac{\partial u^+(x^+, y^+)}{\partial y^+} \tag{16}$$

III. Results And Discussions

The Matlab 7.0 software was used for the numerical simulation. Based on meshes analysis, our choice focused on the mesh (71X51X 31) nodes in order to make a compromise between cost, accuracy and calculation time.The dimensionless geometrical data of the reservoir are given in the following tab. 1 as:

TABLE I. RESERVOIR GEOMETRICAL DATA

$L=5.10^{-3}$m	**$l=10^{-3}$m**	**$H=2.10^{-2}$m**	**T=0.3193s**
$L/D_H=5$	$l/D_H=5$	$H/D_H=5$	$T^+=200$

A. Velocities u^+, v^+, pressure P^+ and Shear stress τ^+ profiles

Fig. 2 shows the profile of the dimensionless velocityu^+ as a function of y^+ for different values of t^+ to x^+ = 10; Fr = 6.32 and Re = 624. From this figure, we observe a semi-parabolic shape, the extremum (peak) of which is at the level of the orifice.On the left side, the absolute value of the dimensionless velocity increases progressively and on the right side it increases sharply.This means that the existence of the orifice causes the acceleration of fluid in the reservoir. The dimensionless velocity u^+ increases with the increase in dimensionless time t^+.

Fig. 3 shows the evolution of the dimensionless velocity v^+ as a function of y^+ for different values from t^+ to x^+ =10; Fr=6.32 and Re=624. We have a parabolic profile of Poiseuille that is to say that module of the dimensionless velocity v^+ is zero on both sides and maximum on axis of the reservoir. The dimensionless velocities u^+ and v^+ have opposite directions. We also note from this figure that the velocity v^+ increases with the time t^+.

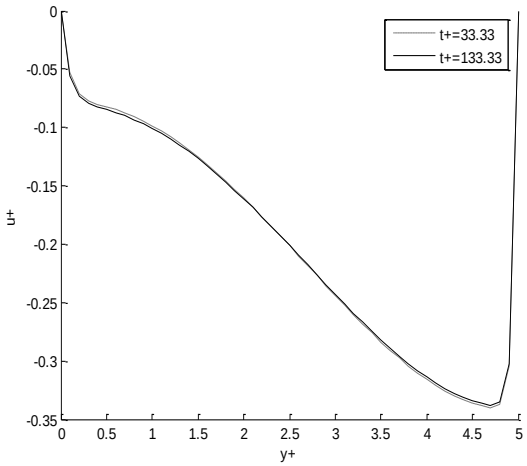

Figure 2.Profile of the dimensionless velocity u^+

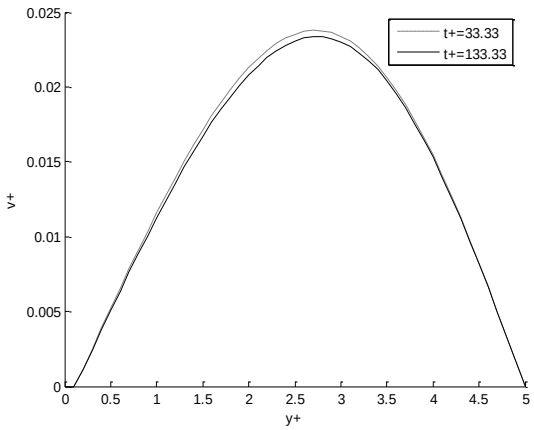

Figure 3.Dimensionless velocity profile v^+

Fig. 4 represents the dimensionless pressure profile P^+ as a function of y^+ for different values from t^+ for x^+ = 10; Fr = 6.32 and Re = 624. We observe that the dimensionless pressure is an increasing function of time and that its profile is comparable to that of the velocity u^+. So we can say that the pressure P^+ and the speed u^+ are proportional.

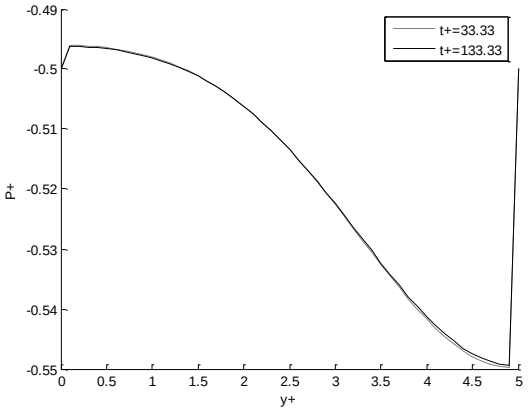

Figure 4. Dimensionless pressure P^+ profile

Fig. 5 gives the evolution curve in absolute value of the dimensionless shear stress τ^+ as a function of the dimensionless width y^+ of the reservoir for x^+ = 10; Fr = 6.32; Re = 624 and t^+ varied. From this curve, we can deduce that the shear stress is maximum on the right wall compared to the left wall while else where it is almost zero. This means that as you move away from the walls, the fluid velocity increases and the shear stress decreases. The shear stress acts as the resistance of the fluid flow. It remains almost constant over time.

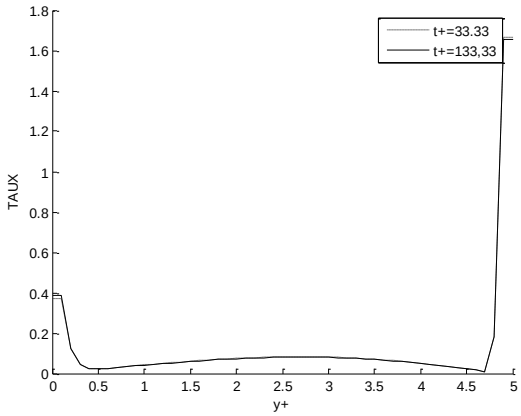

Figure 5. Shear stress profile for t^+ varied

B. Influence of ratio H / L

Fig. 6 shows the evolution of the dimensionless velocity u^+ as a function of y^+ for different values of H / L. We find for x^+ = 10; t^+ = 100; Re = 624 and Fr =

6.32 that the dimensionless velocity u^+ and the H / L ratio are inversely proportional. If the H / L ratio increases, the velocity u^+ decreases and vice versa. The closer you get to the discharge orifice, the greater the dimensionless velocity becomes.

Fig. 7 shows the evolution of the dimensionless velocity v^+ as a function of y^+ for different values of H / L. We find for x^+ =10; t^+= 100; Re = 624 and Fr = 6.32 that the dimensionless velocity v^+ and the H / L ratio are inversely proportional. If the H/L ratio increases, the velocity v^+ decreases and vice versa. The closer one gets to the discharge orifice, the greater the dimensionless velocity becomes very important.

Fig. 8 shows the evolution of the dimensionless pressure P^+ as a function of y^+ for different values of H / L. For x^+ = 10; t^+= 100; Fr = 6.32 and Re = 624, we prove that the dimensionless pressure P^+ increases in proportion to the increase in the height of the reservoir.

Fig. 9 shows the evolution of the dimensionless pressure τ^+ as a function of y^+ for different values of H / L for x^+ = 10; t^+ = 100; Fr = 6.32 and Re = 624. When H / L decreases, the shear stress τ^+ increases. This means that the dimensionless shear stress is proportional to the dimensionless velocity u^+.

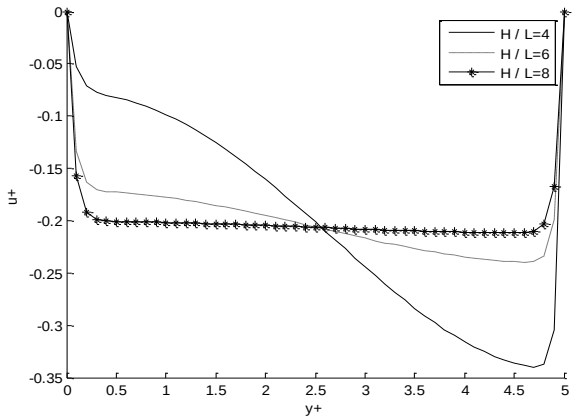

Figure 6.Evolution of the dimensionless velocity u^+ as a function of the dimensionless width y^+ of the reservoir for different values of H / L

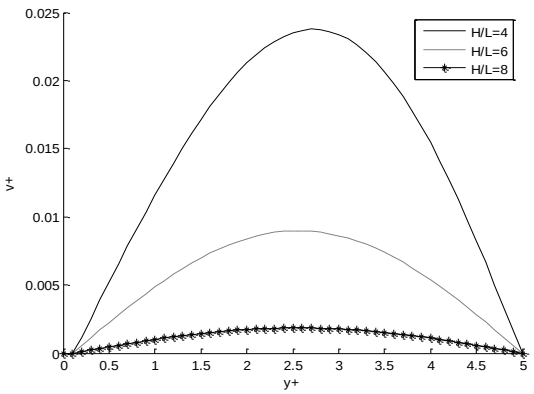

Figure 7.Evolution of the dimensionless velocity v^+ as a function of the dimensionless width y^+ of the reservoir for different values of H / L

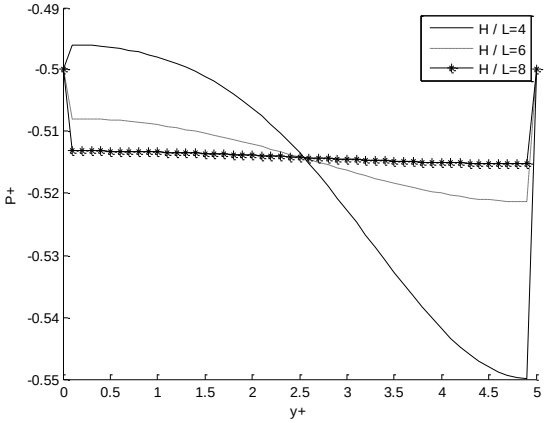

Figure 8.Evolution of the dimensionless pressure P+ as a function of the dimensionless width y+ of the reservoir for different values of H / L

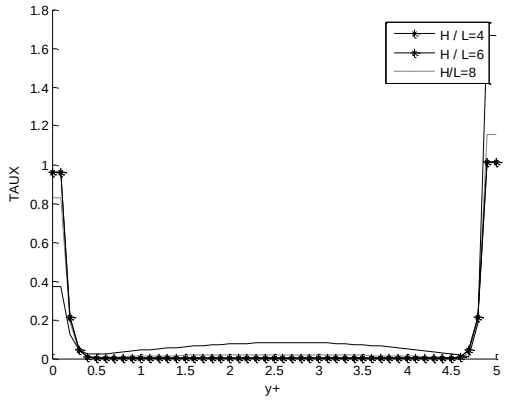

Figure 9.Evolution of the dimensionless shear stress τ+ as a function of the width dimensionless y+ of the reservoir for different values of H / L

C. Reynolds number influence

Fig. 10 shows the profile of the dimensionless velocity u^+ as a function of the dimensionless width of the reservoir y^+ at x^+ = 10; t^+ = 100 and Fr = 6.32 for different Reynolds numbers.We see that the dimensionless velocity u^+ increases proportionally with the Reynolds number. At the orifice, the velocity becomes very important.

Fig. 11 shows the profile of the dimensionless velocity v^+ as a function of the dimensionless width of the reservoir y^+ at x^+= 10; t^+ = 100 and Fr = 6.32 for different Reynolds numbers. We see that the dimensionless velocity v^+ increases proportionally with the Reynolds number.

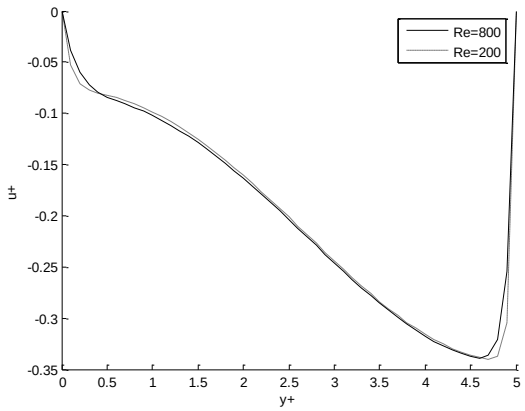

Figure 10. Evolution of the dimensionless velocity u^+ as a function of the dimensionless width y^+ of the reservoir for different Reynolds numbers

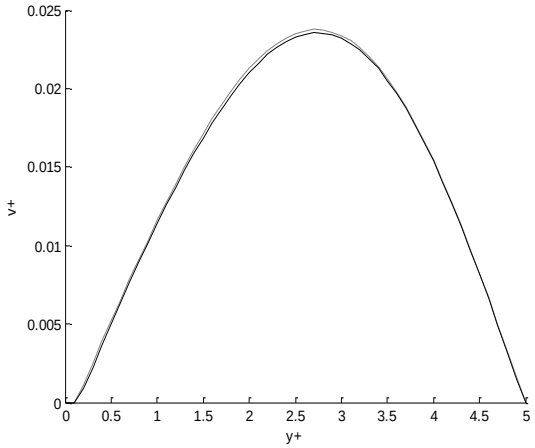

Figure 11.Evolution of the dimensionless velocity v^+ as a function of the dimensionless width $y^+$of the reservoir for different Reynolds numbers

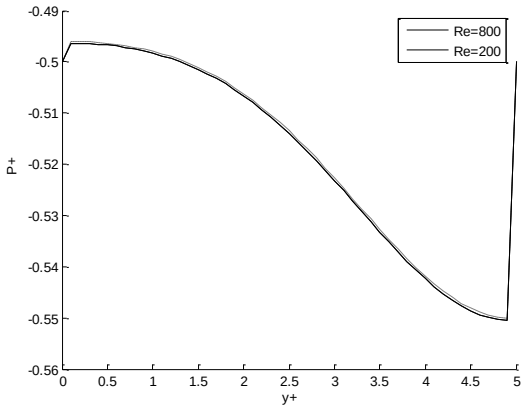

Figure 12.Evolution of the dimensionless pressure P^+ according to the dimensionless width y^+ of the reservoir for various Reynolds numbers.

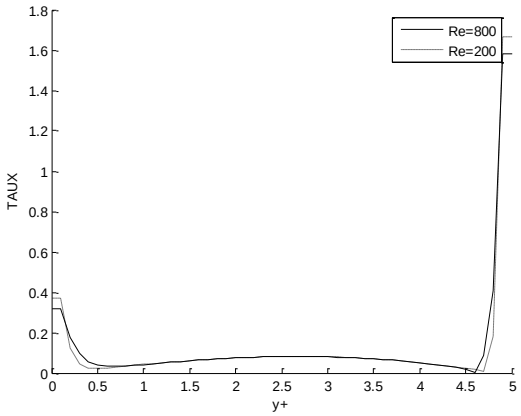

Figure 13.Evolution of the dimensionless shear stress τ^+ as a function of the dimensionless width y^+ of the reservoir for different Reynolds numbers

Fig. 12 shows the profile of the dimensionless pressure P^+ as a function of the dimensionless width of the reservoir at $x^+ = 10$; $t^+ = 100$ and Fr = 6.32 for different Reynolds numbers. We see that the Reynolds number has a small influence on the dimensionless pressure because for Re increases P^+ decreases. So they are inversely proportional.
Fig. 13 represents the profile of the dimensionless shear stress τ^+ as a function of the dimensionless width y^+ of the reservoir at $x^+ = 10$; $t^+= 100$ and Fr = 6.32 for different Reynolds numbers. On both sides, τ^+ varies proportionally with Re, while elsewhere it remains constant.

D. Streamlines

Fig. 14 represents the **S**treamlines or the particles of Newtonian fluid trajectories in the reservoir for $t^+ = 100$. It is well proven from the figure that the fluids converge towards the discharge orifice. There is a recirculation of the fluid on the left corner of the reservoir.

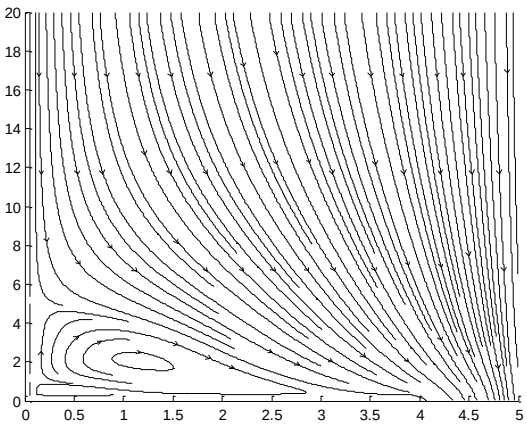

Figure 14. Streamlines in the reservoir

E. Model validation

To validate our model, we will takel=L and H > 10L, that is to say that the width of the orifice and that of the

reservoir are equal. In this case, the reservoir can be regarded as an infinitely long vertical rectangular pipe. Analytically, the velocity of the fluid is given by Poiseuille's law:

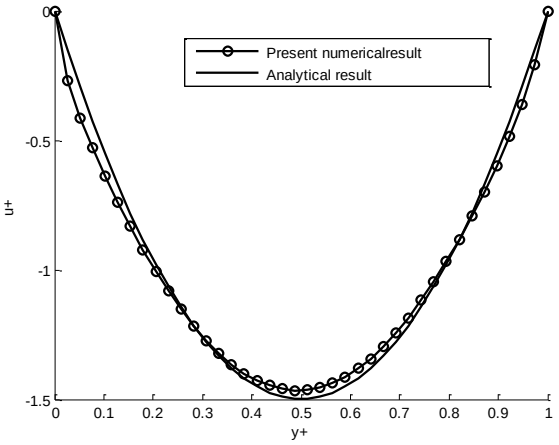

Figure 15.Validation curve

IV. CONCLUSIONS

This work concerns the numerical study of a laminar and unsteady flow of a Newtonian fluid in a rectangular reservoir emptying using an orifice on the right bottom. The conservation of mass and momentum equations were used to model the two-dimensional system. In this case, it was assumed that there are no heat transfers and that the physical properties of the fluid are considered constant. The dimensionless equations thus obtained associated with the boundary conditions are discretized according to the finite volume method. Thomas's algorithm has been used to solve the equations discretized. The velocity-pressure coupling is processed by the SIMPLE algorithm.

The results allow us to visualize the profiles of the velocities u^+ and v^+, pressure P^+, the streamlines and the shear stress τ^+ in the reservoir. The Reynolds number and the H/L, L/l ratios influence on the fluid flow. It can also be seen that the fluid velocity depends on the size of the reservoir such as its height, its width and the width of the orifice.

ACKNOWLEDGMENT

I would like to express my deep appreciation to the team of the Laboratory of Mechanics Energy and Environment (LMEE) for their collaboration.

REFERENCES

[1] C. Yuce, « An Experimental Investigation of Pollutant Mixing and Trapping in Shallow Coastal Re-circulating Flows », *Proceedings*(Juka G H and UijttewaalWs), International Symposium on Shallow flows, Delft, Netherlands 2003, vol. 12, pp. 413-420

[2] G. Forbes, "Unsteady of a fluid from a Circular Tank" Applied Mathematical Modelling, 34(2010), 24,pp.3958-3975

[3] M. Fadhilah « Numerical Simulation of liquids draining from a tank using openFOAM » International Research and Innovation summit,G 22652017), 2, pp1-11.

[4] B. Mathieu, "Numerical Investigation of Flow patterns in RectangularShallow Reservoirs »Engeneering Application of campitational Fluid Mechanics, 2(2011),5, pp.247- 258.

[5] S. Camnasio « Coupling Between Flow and SedimentaDeposition in Rectangular Shallow Reservoirs »Journal of HydraulicReaserch,5(2013), 51, pp.535-54.

[6] S. A. Kantoush, "Channel Formation inLarge Shallow Reservoirswith Different Geometries during Flushing"J. Env. Technology, 30 (2009)34, pp.1020-1032.

[7] T.Taymaz, "Three Dimensional Numerical Modelingof Flow Field in Rectangular Shallow Reservoirs" Proceedings(Schleiss AJ, De Cesare G, Franca M J and PfisterM(Eds) CRC Press),7th River Flow Conference, Lausanne,Switzerland, London, UK, 2010, vol. 2, pp. 11-19

[8] S. Ferrara, « Flow field inshallow reservoir with varying inlet and outlet position » Journal of Hydraulic Research,22 (2018), 5, 1814-1824.

[9] A. Miranda, " Experimental and Numerical Investigation of Flow Patterns in Shallow Rectangular Reservoirs with Symmetrically PositionedInlet and Outlet Channels", Brazilian Journal of Water resources, 23 (2018), 19, pp. 1-12.

[10] J. Peng, "Modeling Free Surface in Rectangular Sallow Basins by Using Lattice Boltzmann Method", Journal of Hydraulic engineering, 137 (2011), 12, pp. 1680 -1685.

[11] Patankar, "Numerical Heat Transfer and Fluid Flow", Ph. D. thesis,Hemisphere,Washington DC,1980.

[12] Versteeg and Malalasekera, "An Introduction to Computational FluidDynamics", Ph. D. thesis,Ed. Longman, England ,1995.